J Nanostruct 15(2): 684-701, Spring 2025

RESEARCH PAPER

Utilization of Green Synthesized Calcium Doped TiO_2 Photocatalysts for the Solar-Light-Driven Degradation of Dyes in Aqueous Solution

Seyed Mehdi Sajjadi *, Ghader Hosseinzadeh

Department of chemical Engineering, University of Bonab, Bonab, Iran

ARTICLE INFO

Article History:
Received 27 January 2025
Accepted 26 March 2025
Published 01 April 2025

Keywords:
Ca-doped TiO_2
Green sol-gel
Photocatalyst
Water treatment

ABSTRACT

In this study, Ca-doped TiO_2 photocatalysts with various amounts of Ca (0, 3 and 5 wt. %) and also utilization of Cannabis Sativa leaves were synthesized by green sol-gel method. Afterward, physicochemical properties of the photocatalysts were assessed by XRD, FESEM, EDAX, TEM, BET, FTRI and DRS analysis. Next, prepared photocatalysts were applied in photocatalytic degradation of Methylene Blue (MB) and Rhodamine B (RhB) under the simulated sunlight illumination. Among the prepared photocatalysts, 5 wt. % Ca-doped TiO_2 (CaTi5) photocatalyst demonstrated the excellent characterizations such as higher surface area, smaller particles size and uniform dispersion and lower energy band gap. CaTi5 based on the superior characterizations indicated the highest dyes degradation. MB and RhB degradation for the CaTi5 after 240 min simulated sunlight illumination were 85% and 90%, respectively. Also, photocatalytic dyes degradation were in agreement with the pseudo first-order reaction kinetic. Moreover, among the various concentrations of CaTi5 (50, 75, 100, 125 and 150 ppm) highest amount of degradation was found for 100 ppm catalyst concentration. Therefore, we can say that CaTi5 is a promising photocatalyst for solar-light-driven degradation of MB and RhB in aqueous solution.

How to cite this article
Sajjadi SM., Hosseinzadeh G. Utilization of Green Synthesized Calcium Doped TiO_2 Photocatalysts for the Solar-Light-Driven Degradation of Dyes in Aqueous Solution. J Nanostruct, 2025; 15(2):684-701. DOI: 10.22052/JNS.2025.02.027

INTRODUCTION

Today, providing of drinking water and treatment of wastewater is one of the major concerns of the world community [1, 2]. Various types of hazardous chemical matters are involved in the pollution of water resources. One of these hazardous materials is synthetic dyes. Owing to the literature, approximately 280000 tons of textile dyes such as methylene blue (MB) and rhodamine B (RhB) are discharged as industrial effluent each year [3]. Mentioned dyes which originated from industries such as textiles, leather, paper and pharmaceuticals are very harmful for human health [4]. Moreover, the existence of dyes in water by reduction of the sunlight penetration in water caused the weaken photosynthesis power of aquatic plants [5, 6]. Owing to the conducted research, dye degradation techniques are includes three main groups. The first group is physical methods such as adsorption and ion exchange approaches. The second group is chemical methods including ozonization and

---

* Corresponding Author Email: Mehdi_sajjadi@ubonab.ac.ir

photocatalytic reactions and finally, third group is biological methods such as aerobic and anaerobic degradation [7, 8]. Among the cited methods, dyes degradation by the photocatalysts due to it’s the advantages such as environmental preservation, perfect removal of pollutants and no subordinate pollution, has attracted a lot of much attention [9-11]. In this field of study, TiO_2 photocatalyst, due to its cheapness, non-toxicity, fast reactions and high-efficiency ability to absorb pollutants and dye removal from contaminated water, has received more attention [12-14]. The size of the TiO_2 particles is an important factor that influences the characterizations of photocatalysts. Thus, several studies by various researchers were conducted in the case of particle size and synthesis methods of photocatalysts [12, 15, 16]. Among the various methods, the sol-gel technique, owing to low temperature processing and also the ability to control the particles size and morphology, has been employed extensively in nanocatalysts fabrication [17, 18]. However, TiO_2 is an appropriate candidate for photocatalytic dye degradation, but some major drawbacks remain. The first problem is related to the high energy band gap of TiO_2 which for its exciting, large amount of energy is required. Secondly, the lower speed of electron transfer to oxygen and higher speed of electron-hole recombination lead to a lower quantum yield rate and restricted photo-oxidation rate [19]. For solving the noted problems, we can use of strategies such as heteroatoms doping and also, heterojunctions construction. Anatase TiO_2 was doped with Mn^{2+}, Ni^{2+} and Zn^{2+} and they applied for photocatalytic removal of Aniline Blue by solar light. Among them, Mn-doped TiO_2 presented the higher activity [20]. Zhu and coworkers studied the catalytic performance of Cr-doped TiO_2 and pure TiO_2 during the degradation of active yellow XRG. It was found that, 0.15 wt.% Cr-doped TiO_2 exhibited the smaller crystal size, greater surface area and also, higher degradation [21]. Based on the literature among the C, N, F, P and S, nitrogen was the most effective dopant for enhancement of the photocatalytic performance of TiO_2 [22, 23]. Liu and et al. evaluated the MB degradation by TiO_2/g-C_3N_4 heterojunction photocatalysts. They reported higher amount of dye degradation for heterojunction composite in comparison with individual TiO_2 and g-C_3N_4 nanocatalysts [24]. Ag@TiO_2/WO_3 heterojunction photocatalyst illustrated higher photocatalytic degradation of MB in comparison with TiO_2, WO_3 and TiO_2/WO_3 [25]. Moreover, better performance of the TiO_2 based heterojunction photocatalysts was presented for SnO_2-TiO_2 [26], NiO-TiO_2 [27] and BiOI-TiO_2 [28]

Table 1. Physicochemical properties of methylene blue and Rhodamine B.

Organic Dye	Chemical Formula	Chemical Structure	Molecular Weight (g/mol)	Solubility in Water (mg/mL)	λ_{max} (nm)
Methylene Blue	$C_{16}H_{18}ClN_3S$	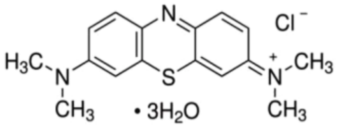	**319.85**	**43.6**	**665**
Rhodamine B	$C_{28}H_{31}ClN_2O_3$	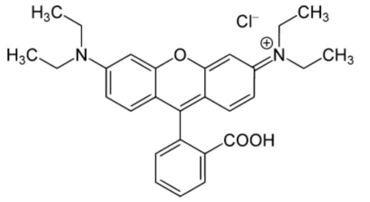	**479.02**	**50**	**552**

heterojunctions. In the photocatalysts preparation procedures, a series of special considerations such as elevated temperatures, expensive precursors and toxic materials were required. Therefore, green synthesis methods were emerged. During this technique sustainable materials like plant extracts, microorganisms and enzymes were applied. Therefore, the safety of the synthesized materials was improved and procedure costs were diminished [29, 30]. Beta vulgaris peel extract was used in the green synthesis of Ag/TiO_2 photocatalyst by Jayapriya and coworkers. They reported degradation efficiency of 92% for MB [31]. In another study [32] copper promoted TiO_2 particles by use of the C. benghalensis plant extracts were fabricated and applied for photocatalytic degradation of MB, ciprofloxacin and sulfisoxazole. The greatest degradation (94%) was gained by sulfisoxazole [32]. Here in this research, the use of Cannabis Sativa (CS) in the synthesis of calcium doped TiO_2 photocatalysts is reported for the first time to the best of our knowledge. Therefore, in this study, Ca-doped TiO_2 photocatalysts with various amounts of Ca and also, utilization of Cannabis Sativa (CS) leaves were synthesized with green sol-gel method. In the following, fabricated photocatalysts were assessed by XRD, FESEM, EDAX, TEM, BET, FTRI and DRS analysis. Next, prepared photocatalysts were applied in photocatalytic degradation of Methylene Blue (MB) and Rhodamine B (RhB) under simulated sunlight illumination.

MATERIALS AND METHODS

Materials

During the synthesis procedure of nanocatalysts, $Ca(NO_3)_2.4H_2O$ and Titanium tetra-isopropoxide (TTIP) were applied as Ca and Ti, precursors, respectively. Ethanol was used as solvent. MB and RhB were employed as organic dye pollutants and their specifications were illustrated in Table 1. All dyes and precursors were purchased from

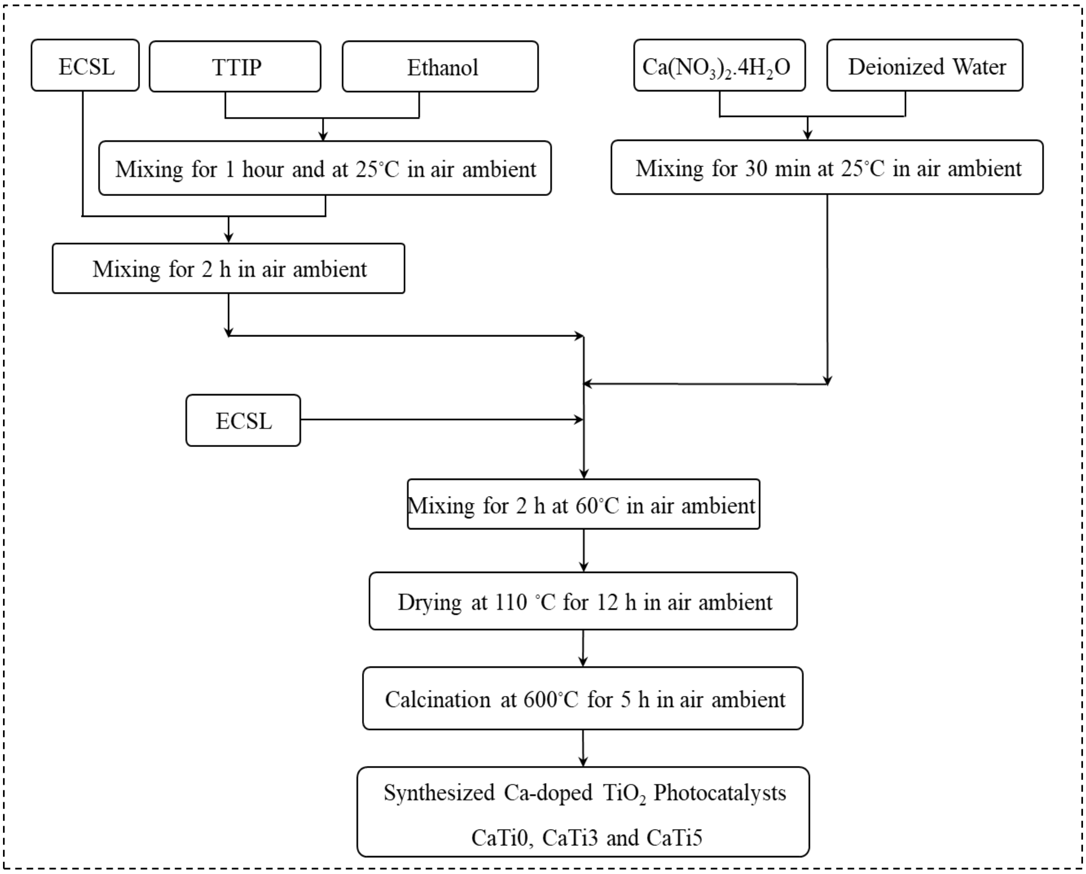

Fig. 1. Synthesis diagram of the Ca-doped TiO_2 photocatalysts.

the Merck Company. Deionized water was used as solvent in all experiments. CS leaves were collected from East Azerbaijan.

Preparation of Extract

First, 10mg of CS leaves were gathered and next, to remove of the contamination on the leaves, they were cleaned with water. In the following, the leaves were dried in air and then were cut down into the fine pieces. Next, they were poured in 100 mL of deionized water and heated at in 60°C for one hour. Extracted from CS leaves (ECSL) which was a light brown solution, was centrifuged for 15 min at 4000rpm. The upper clear part was separated and used in the following.

Synthesis of photocatalysts

The synthesis procedure of the Ca-doped TiO_2 photocatalysts with green sol-gel method was presented in Fig. 1. At first, the appropriate amount of TTIP was stirred in 50 ml of ethanol for 1h and at 25°C. Next, 10 ml of ECSL was added to a homogenous solution of TTIP in dropwise manner and mixing was go on for 2h. Besides the noted steps, an appropriate amount of calcium nitrate tetra hydrate was solved in deionized water and added to the TTIP and ECSL solution. Next, another 5 ml of ECSL was drop-wisely introduced to the solution. Obtained solution was stirred for another 2h and at 25°C. next, the solution was cool down. In the following, solution was centrifuged for 15 min at 4000 rpm. Solid product at the bottom of the vials was washed with deionized water for twice. Next, it was dried at 110°C for 12h and was calcined at 600°C for 5h. The obtained powder were Ca-doped TiO_2 photocatalysts. Calcium doped TiO_2 photocatalysts with 0, 3 and 5 wt.% were denoted as CaTi0, CaTi3 and CaTi5, respectively.

Photocatalysts characterization technique

XRD patterns of photocatalysts were evaluated by Philips X' Pert MPD with Cu Kα radiation (λ= 0.15406 nm). MIRA3 TESCAN used as FESEM and EDAX analysis devise for investigation of the surface morphology of photocatalysts. Moreover, FTIR test (400-4000 cm^{-1}) by utilization of Shimadzu IRAffinity-1S was applied to the study of the functional groups. Also, surface area measurement of the fabricated nanocatalysts was done with Quantachrome chembet-3000 during the BET analysis. Diffuse reflectance spectroscopy (DRS) was done via utilization of the Shimadzu UV-2550 UV–vis spectrophotometer. The applied wavenumber was between 200-600 nm.

Photocatalytic activity

Photocatalytic performance of the fabricated photocatalysts during the degradation of dyes under simulated sunlight illumination was carried out with utilization of the 100 mg/L of photocatalysts. The above-noted sample was suspended in a 200 mL dye aqueous solution which was contained 5 ppm dye. Prior to the performance evaluation under the simulated sunlight, adsorption/desorption equilibrium was required. This goal was achieved by stirring the mixture of photocatalyst and dye solution in the dark ambient and for 1h. After assessment of the results of the dark test, the mixture was tested under the light of a 400 W halogen lamp, manufactured by OSRAM in Germany, for 240 min. Each 30 min, 5 mL of aqueous solution was caught as a sample and instantly centrifuged. Separated dye solutions (without photocatalysts) were tested with UV–Vis spectrophotometer at the maximum wavelengths of 665 and 552 nm for MB and RhB, respectively. Photo degradation efficiency (PDE) of dyes was calculated by the following equation.

$$\text{PDE}\ (\%) = (1-\frac{C_t}{C_0})*100\% \quad (1)$$

In the cited equation, C_0 (mg/L) was concentrations of MB or RhB before illumination. Also, C_t was the concentration at time t after illumination (mg/L).

RESULTS AND DISCUSSION

Photocatalysts characterizations

XRD analysis

XRD patterns of the Ca-doped TiO_2 photocatalysts synthesized by green sol–gel method, at 2θ=20-80° were illustrated in Fig. 2. Some peaks at 25.33, 36.01, 37.90, 48.06, 53.96, 55.06, 62.70, 69.01, 70.41 and 75.32° were detected that belong to these planes (101), (103), (004), (200), (105), (211), (204), (116), (220) and (215). Comparing the presented peaks with the literature proved that the formed structure was ascribed to the anatase phase of TiO_2. This formation was proved by matching of the obtained results with JCPDS card No. 84-1285 [33]. Comparing the patterns of the pure TiO_2 and Ca doped ones indicated that there was no CaO peaks in the obtained patterns. Therefore, we can say that Ca^{2+} ions probably have been completely integrated into the TiO_2 crystal lattice and also, calcium was dispersed more uniformly in the structure of photocatalysts. It must be noted that since CaO peaks were not detected in XRD patterns, the existence of the calcium in the structure must be proven in some way. This matter will be discussed in EDAX analysis. Generally, by increasing the Ca loadings the intensity of peaks was reduced and the peaks became broader. Thus we can say that for the Ca-promoted photocatalysts the crystal size was reduced and the uniform dispersion was enhanced. This trend is in line with the other studies [34, 35].

FESEM analysis

FESEM images of Ca-doped TiO_2 photocatalysts were presented in Fig. 3. Based on the images, calcium addition to the pure TiO_2 led to the uniform dispersion and roughly smaller particles size. Moreover, by rising of the Ca loadings, uniform dispersion has been intensified. Owing to the smaller particles size and uniform morphology of the Ca-doped TiO_2 photocatalysts, displaying of the higher surface area for the CaTi3 and CaTi5 is probable. This claim will be evaluated in the BET analysis. Uniform dispersion of Ca-doped photocatalysts was probably ascribed to the applied synthesis method and the nature of the calcium precursor. In sol-gel method growth of particles and condensation rate belong to the nature of synthesis media (acidic or basic condition). It is probable that by increasing the Ca loadings and subsequently ascending of the applied $Ca(NO_3)_2.4H_2O$, formation of nitric acid was developed. Thus, by increasing the Ca content, the acidity of synthesis media was increased and led to the higher speed of hydrolysis step, more stable sol and finally smaller particles size and more uniform dispersion [36]. However, the uniform dispersion was consistent with the rising calcium content, but further calcium increase might lead to the some disadvantages. Due to the greater ionic radius of Ca in comparison with Ti, it was probable that the addition of further amounts of Ca (higher than 5

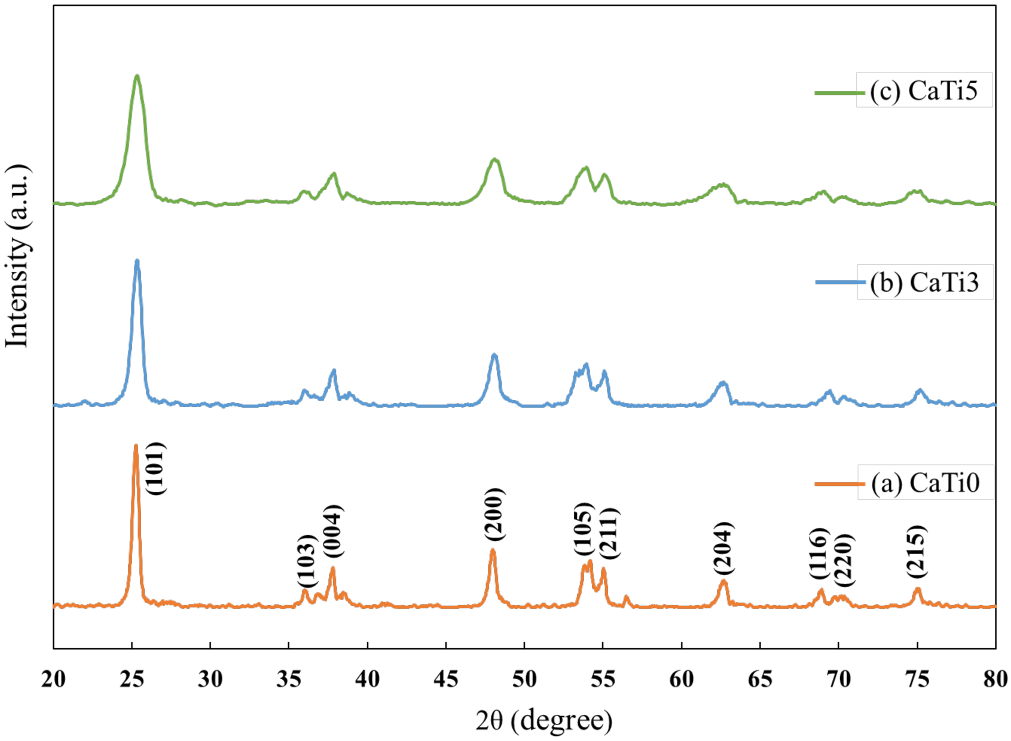

Fig. 2. XRD patterns of the Ca-doped TiO_2 photocatalysts.

wt.%) caused the pores blockage, agglomeration and finally non-uniform dispersion and lower surface area.

EDAX analysis

Results of EDAX analysis of CaTi0, CaTi3 and CaTi5 were shown in Fig. 4. As displayed in images all the constituent elements of the photocatalysts were detected in the final structure of the catalysts. Thus, EDAX analysis verified the existence and dispersion of Ti and O in the structure of CaTi0 and also, Ti, Ca and O in the structures of the CaTi3 and CaTi5 photocatalysts. Therefore, the cited problem in the case of no observation of CaO in XRD patterns was solved. Moreover, images indicated that by increasing of Ca contents, dispersion was improved and uniform morphology was obtained. Furthermore, in the case of Ca-rich photocatalysts dispersion without agglomeration (or with lower amount) was exhibited. These results are in agreement with XRD and FESEM analysis.

TEM analysis

In order to further morphological investigation of the fabricated photocatalysts, TEM analysis was performed and the TEM image of the 5 wt.% Ca-

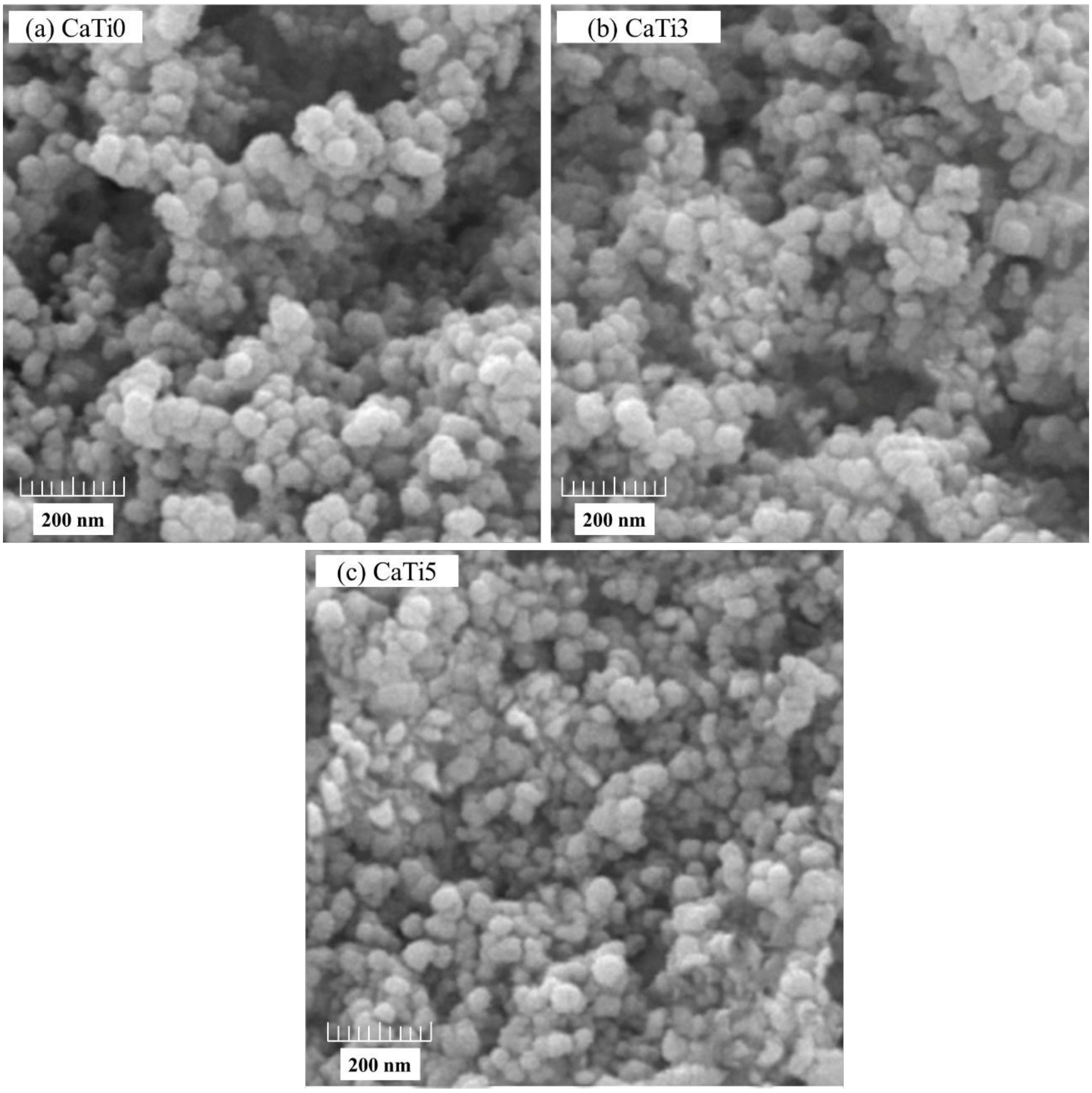

Fig. 3. FESEM images of the Ca-doped TiO_2 photocatalysts.

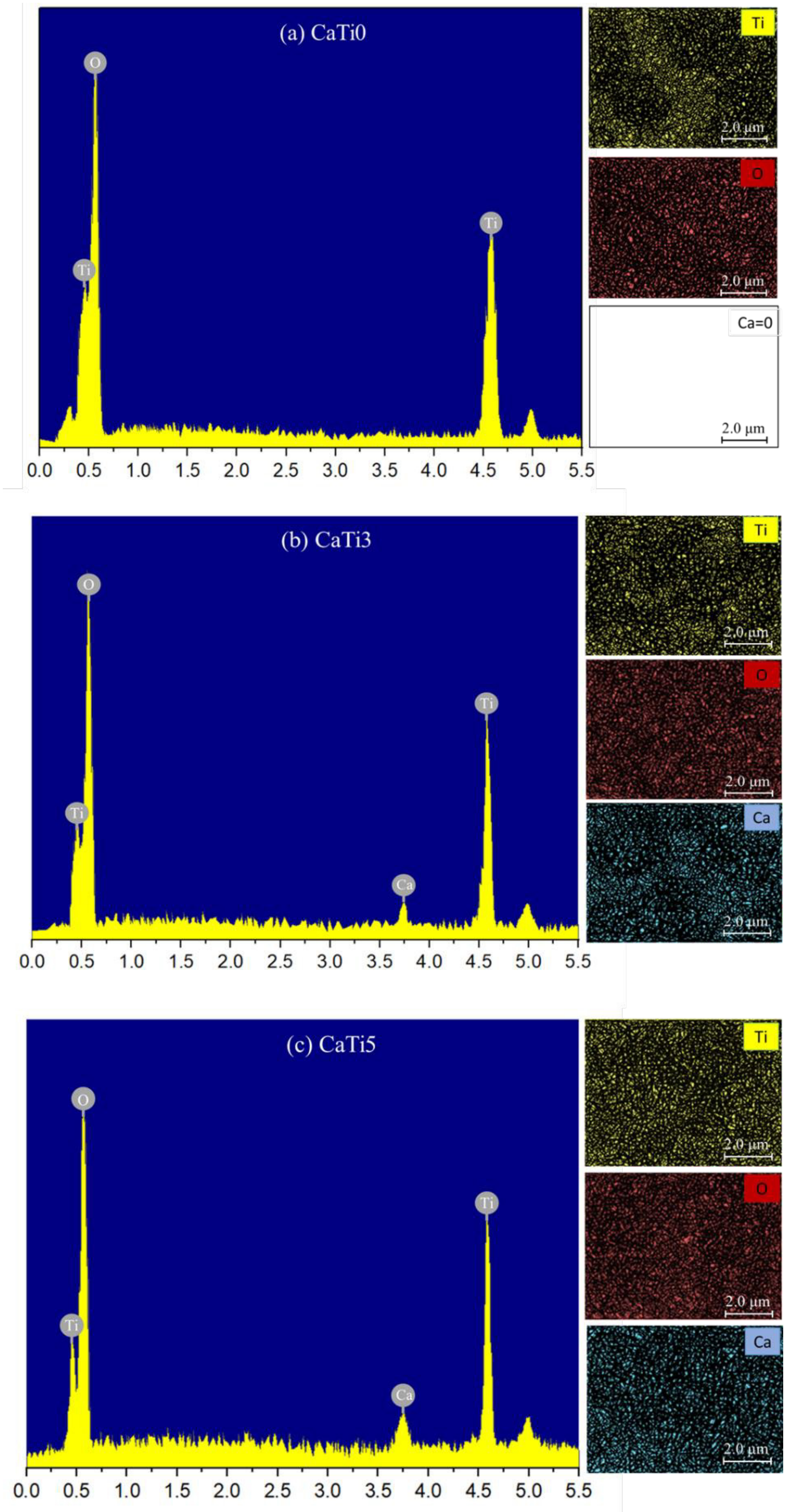

Fig. 4. EDAX analysis of the Ca-doped TiO_2 photocatalysts.

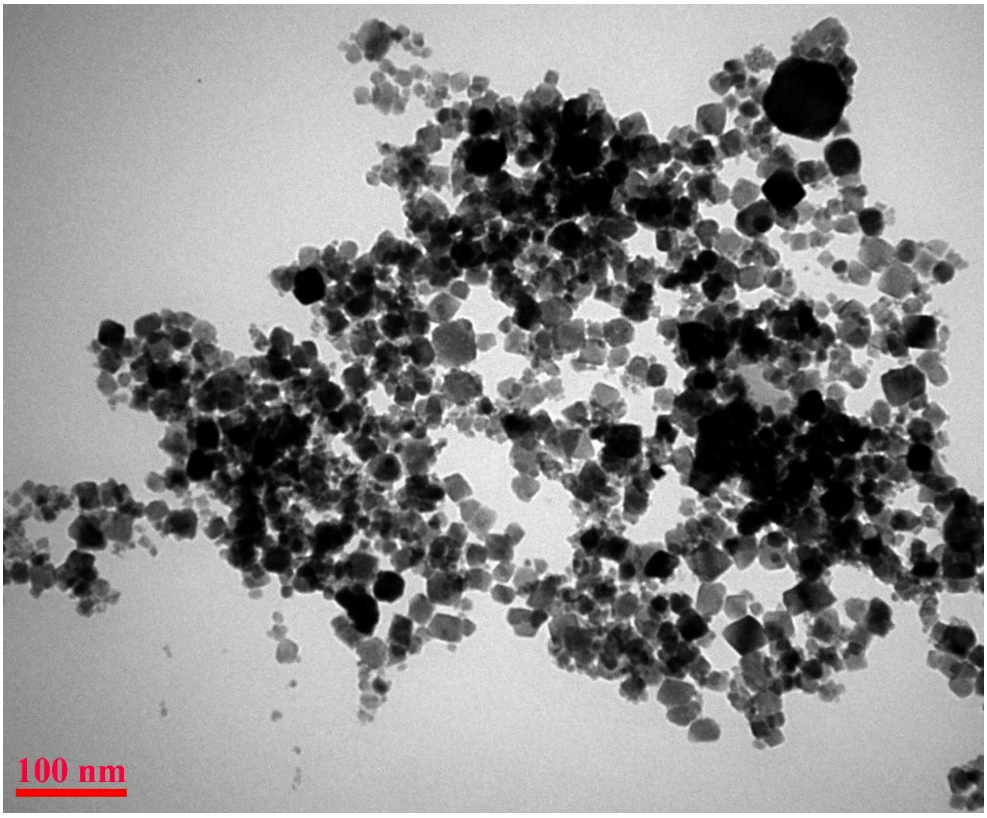

Fig.5. TEM images of Ca-doped TiO_2 photocatalyst: CaTi5.

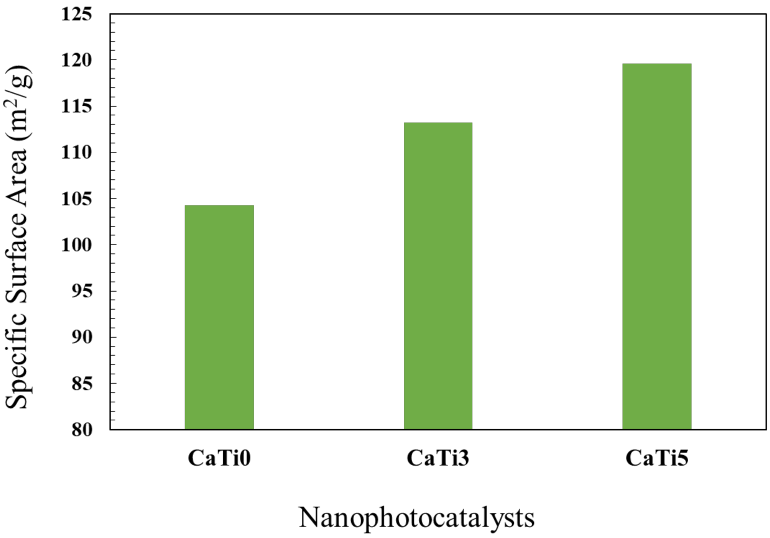

Fig. 6. BET analysis of the Ca-doped TiO_2 photocatalysts

doped TiO_2 photocatalyst was depicted in Fig. 5. As can be seen, most of the metallic particles are less than 50 nm. Qualitatively, tiny metallic particles, uniform distribution of particles size and excellent metallic dispersion can be evidenced for CaTi5. Fine and uniform metallic particles probably lead to the higher surface area and superior photocatalytic performance. Exhibited features are in line with FESEM and EDX analysis.

BET analysis

Results of the BET analysis of Ca-doped TiO_2 photocatalysts were presented in Fig. 6. Surface area for the CaTi0, CaTi3 and CaTi5 were 104.3, 113.2 and 119.6m^2/gr, respectively. Owing to the mentioned data, Ca addition caused the higher surface area for the Ca-doped TiO_2 photocatalysts and also, the greatest amount was gained for the CaTi5. This trend was ascribed to the more uniform dispersion and smaller particles size of the Ca-doped ones in comparison with pure TiO_2 and is in line with results of FESEM analysis. Owing to the literature, the rates of dye degradation by the heterogeneous photocatalysts and also the adsorption ability of photocatalysts are proportional to the specific surface area [37]. Therefore, the highest amount of dyes degradation might be offered by Ca-rich photocatalysts. This claim will be evaluated in the photocatalytic performance section.

FTIR analysis

Fig. 7 shows the FTIR test of the Ca-doped TiO_2 photocatalysts. The functional groups on the surface were evaluated in the range of 400– 4000 cm^{-1}. Peaks which were detected in the range of 450-800 cm^{-1} were related to the Ti–O, Ti–O–Ti and Ca–O bonds [38, 39]. The peaks which were exhibited at 1640 and 3450 cm^{-1} were belong to the OH group [40]. Also, the further peak which was detected at 2350 cm^{-1} was related to the asymmetric stretching frequency of C=O. This vibration might be originated from the aerial CO_2 [41]. Almost the same diagrams were found for

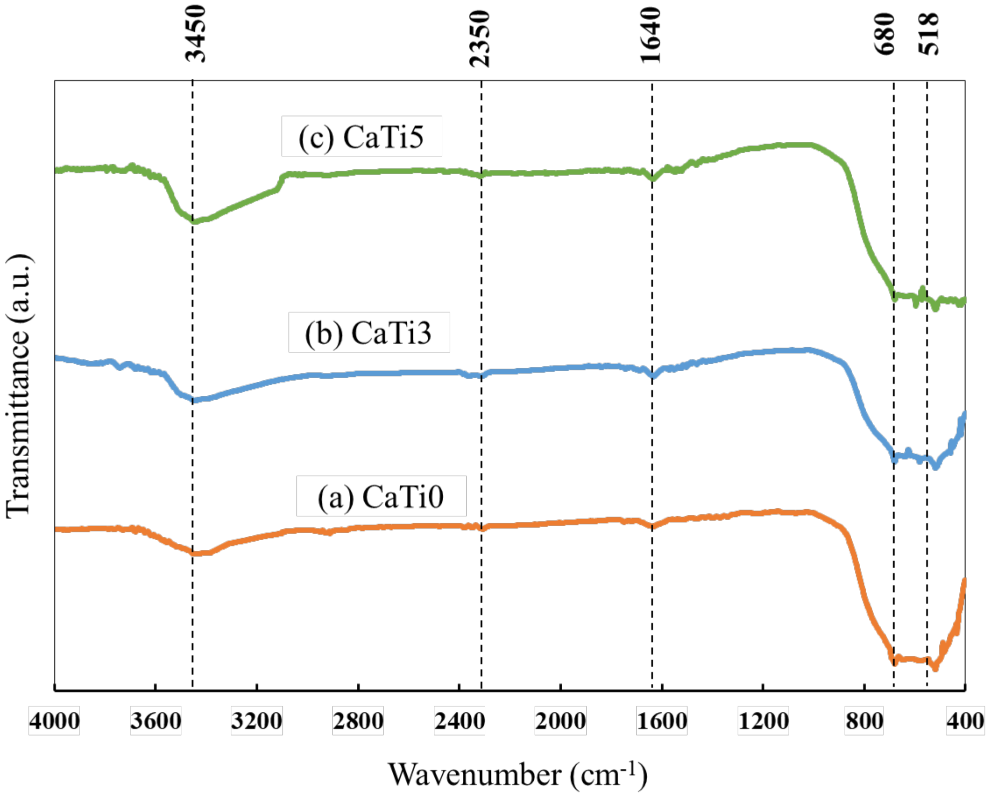

Fig. 7. FTIR analysis of the Ca-doped TiO_2 photocatalysts.

all of the synthesized photocatalysts. The main difference of them was related to the OH groups especially the one which was exhibited at 3450 cm^{-1}. We can say that increasing the calcium loadings led to the higher intensity of OH groups. Moreover, matching the FTIR spectra of the fabricated photocatalysts proved that the greatest OH peak was found for CaTi5. Higher amounts of surface OH groups by intensifying the trapping of electrons caused the improved separation yields of electron-hole pairs. Moreover, it must be noted that the development of surface free radicals (OH), led to the intensified photocatalytic degradation of dyes [42, 43].

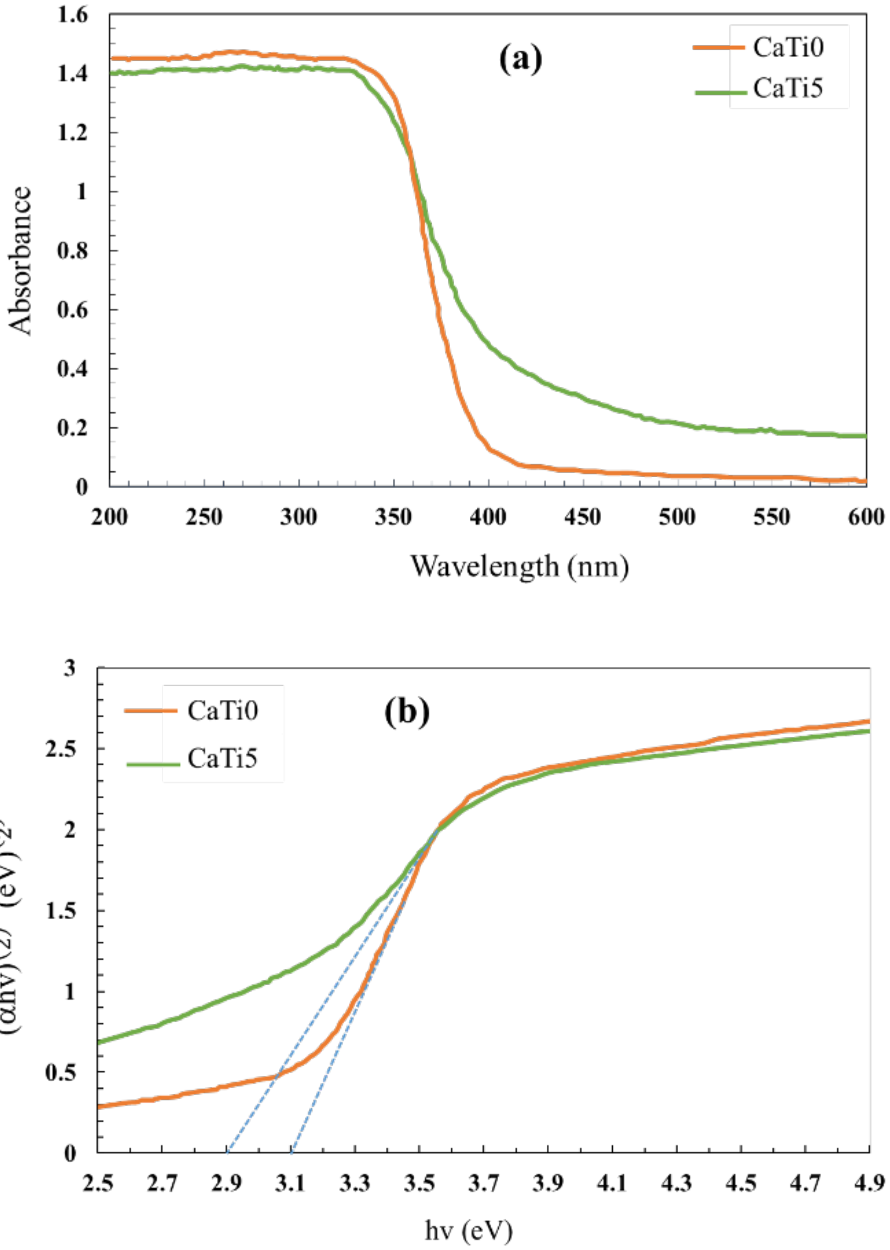

Fig. 8. (a) UV–Vis diffuse reflectance spectra and (b) Tauc plots for Ca-doped TiO_2 photocatalysts.

DRS analysis

To evaluate energy structure and optical properties of the Ca-doped TiO_2 photocatalysts, DRS tests were done and results were presented in Fig. 8. Owing to the absorbance variation versus wavenumber (Fig. 8 (a)) was found that the absorption edges of CaTi0 and CaTi5 were about 395 and 420 nm, respectively. Thus, pure TiO_2 mostly adsorb ultraviolet light. Moreover, Ca addition shifted the absorption edge of the pure TiO_2 to the visible light. The noted shift probably promotes the photocatalytic performance of the Ca-doped TiO_2 photocatalysts under visible light, which will be evaluated in the photocatalytic performance section. Band gap energy (Eg) calculation for the Ca-doped TiO_2 photocatalysts, was possible by plotting of $(\alpha h\nu)^{(1/2)}$ against photon energy (hv). Therefore, the noted graphs were drawn in Fig. 8(b). In the cited diagrams a, h, and v were the absorption coefficient, Plank constant and light frequency, respectively. Based on Fig. 7(b), the energy band gap of the CaTi0 and CaTi5 were 3.1 and 2.9 eV, respectively. Reduction of the energy band gap for the Ca-doped TiO_2 photocatalyst was in line with the trend of adsorption edge and might cause the intensified photocatalytic activity under the simulated sunlight illumination. Also, various amounts of band gap from the different studies were extracted and presented in Table 2. Owing to the obtained data, the band gap of the pure anatase TiO_2 is close to 3.1 eV which is in line with the calculated one [44, 45]. Moreover, comparing the Ca-doped TiO_2 catalysts with various Ca loadings and also various synthesis methods revealed that, band gap of 5 wt.% Ca-doped TiO_2 photocatalyst was probably in the range of 2.85 eV to 2.95 eV [44, 46]. Calculated band gap in this paper was 2.9 eV which is logical and in agreement with previous studies. Moreover, the reported band gap in this paper was lower

Table 2. Comparison the band gap of Ca-doped TiO_2 photocatalysts with previous studies.

No	Material	Synthesis method	Band gad (eV)	Ref.
1	Pure TiO_2	Sol-gel	3.37	[44]
2	1% wt. Ca-dope TiO_2	Sol-gel	3.25	[44]
3	2% wt. Ca-dope TiO_2	Sol-gel	3.2	[44]
4	3% wt. Ca-dope TiO_2	Sol-gel	3.1	[44]
5	Pure TiO_2	Solid state reaction route	3.15	[46]
6	0.88 % wt. Ca-dope TiO_2	Solid state reaction route	3.13	[46]
7	1.33 % wt. Ca-dope TiO_2	Solid state reaction route	3.08	[46]
8	1.59 % wt. Ca-dope TiO_2	Solid state reaction route	3.05	[46]
9	1.87 % wt. Ca-dope TiO_2	Solid state reaction route	2.99	[46]
10	Pure TiO_2	Green synthesis	3.04	[51]
11	Pure TiO_2	Green synthesis	3.1	[45]
12	Pure TiO_2	Green synthesis	3.1	This study
13	3 % wt. Ca-dope TiO_2	Green synthesis	2.9	This study

than the similar papers, which proves the better performance of the applied synthesis procedure.

Photocatalytic degradation of MB and RhB

Influence of photocatalyst type

Photocatalytic performance of the fabricated Ca-doped TiO_2 photocatalysts during the degradation of MB and RhB in the form of relative concentration (C_t/C_0) as a function of illumination time (for 240 min) were assessed and displayed in Fig. 9. Prior to the degradation test of each catalyst, adsorption of the dyes was investigated for 60 min in dark condition. As exhibited in diagrams, approximately 10% degradation took

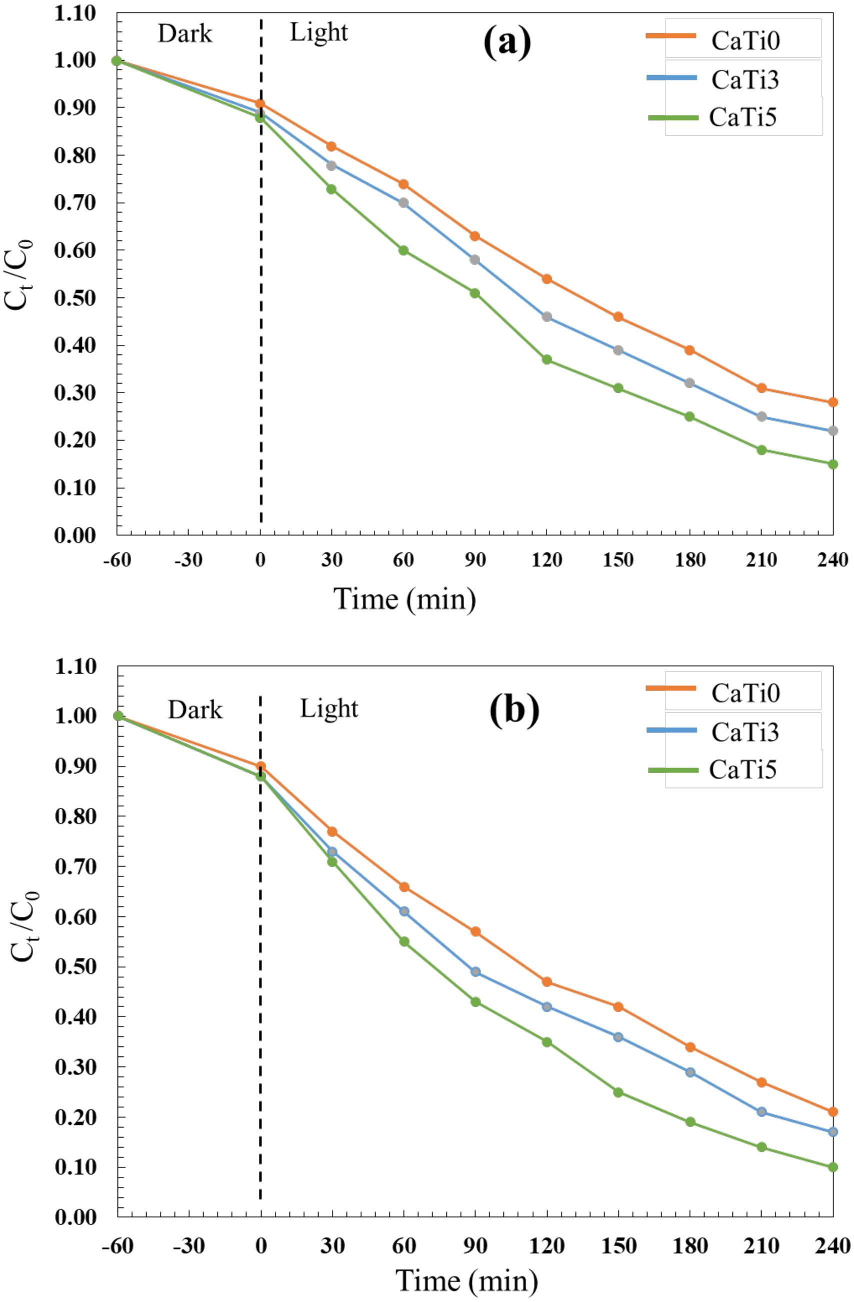

Fig. 9. Photocatalytic degradation of (a) MB and (b) RhB over the Ca-doped TiO_2 photocatalysts.

place during the dark tests for all of the prepared photocatalysts. Generally. We can say that for both dyes, the rate of degradation for Ca-doped photocatalysts was greater than CaTi0. Moreover, by increasing Ca loadings, photo degradation efficiency (PDE) was promoted and CaTi5 presented the highest MB and RhB degradation among the fabricated photocatalysts. PDE of MB and RhB for CaTi5 after 240 min simulated sunlight illumination were 85% and 90%, respectively, while the PDE of MB and RhB for pure TiO_2 were 72% and 79%, respectively. Moreover, calculated results proved that Ca-doped TiO_2 photocatalysts presented the higher photocatalytic degradation efficiency for RhB dye in comparison with MB dye. The better efficiency of the CaTi5 was ascribed to the superior characterizations such as higher surface area, smaller particles size and uniform dispersion, higher ability to form of surface free radical (OH) and lower energy band gap. However, obtained results proved that increasing Ca amounts led to superior catalytic properties and improved photocatalytic activity, but it seems that Ca addition more than 5 wt.%, may cause some drawbacks. Extra addition of Ca might be led to agglomeration, pore blockage, lower surface area, non-uniform dispersion and consequently restrained photocatalytic activity. Thus, it seems that adding only a lower amount of Ca (less than or equal to 5 wt.%) to the pure TiO_2 is appropriate.

Kinetic study

In this section, kinetics of photocatalytic degradation of RhB and MB over the fabricated photocatalysts were studied. In this assessment, Ln (C_0/C_t) versus time (equation No. 2) based on the Langmuir-Hinshelwood model were drawn for all photocatalysts and were displayed in Fig. 10. Plotted charts proved that the degradation kinetics of MB and RhB were matched with pseudo-first-order model.

$$\mathrm{Ln}\left(\frac{C_t}{C_0}\right)=k_{app}*t \qquad (2)$$

Next, based on the pseudo first-order the apparent reaction rate constants (k_{app}) and also, the correlation coefficient (R^2) for all of the fabricated catalysts were calculated and listed in Table 3. The photocatalytic degradation rate (k_{app}) ascended by rising of Ca loadings and the CaTi5 exhibited the higher degradation rate.

Influence of Photocatalyst concentration

Owing to the influence of photocatalysts concentration on the efficiency of the wastewater treatment, in this section various concentrations of CaTi5 (50, 75, 100, 125 and 150 ppm) were applied during the dyes degradation and results exhibited in Fig. 11. As illustrated in graphs for both MB and RhB, the highest amount of degradation was found for 100 ppm catalyst concentration. PDE of MB and RhB for 100 ppm CaTi5 after 240 min test were 85% and 90%, respectively. Lower efficiency for concentration less than 100 ppm might be ascribed to the lower number of active sites and consequently lower reaction rate. For

Table 3. Correlation coefficients and rate constants for MB and RhB photodegradation.

Sample	MB		RhB	
	k_{app}	R^2	k_{app}	R^2
CaTi0 (pure TiO_2)	0.0048	0.9845	0.0056	0.9874
CaTi3	0.0057	0.9868	0.0065	0.9903
CaTi5	0.0072	0.9922	0.0086	0.9923

higher photocatalyst concentration, particles agglomeration and light scattering was possible. Thus, lower efficiency in the case of 125 and 150 ppm, was probably originated from the noted parameters.

Suggested photodegradation mechanism

The mechanism of the photocatalytic

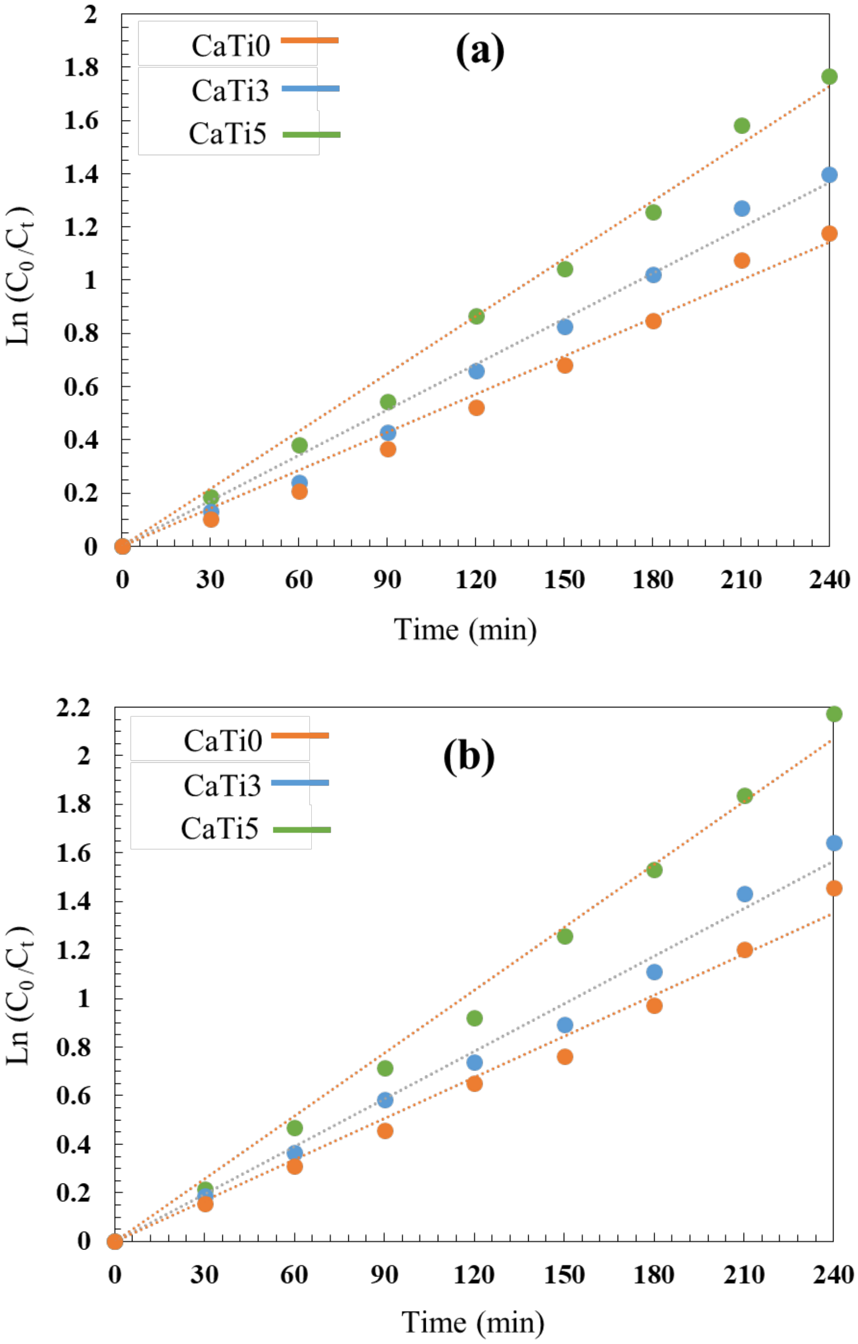

Fig. 10. Pseudo-first-order kinetics of degradation of (a) MB and (b) RhB over the Ca-doped TiO_2 photocatalysts.

degradation of organic pollutants, including dyes is usually initiated when an electron passes from the valence band (BV) to the conduction band (BC), creating a hole (h^+) and an electron (e^-) [47], as represented in Eq. 3.

$$\text{Photocatalyst (Ca-TiO}_2\text{)} + h\nu \rightarrow \text{Ca-TiO}_2 + e^-_{BC} + h^+_{BV}$$

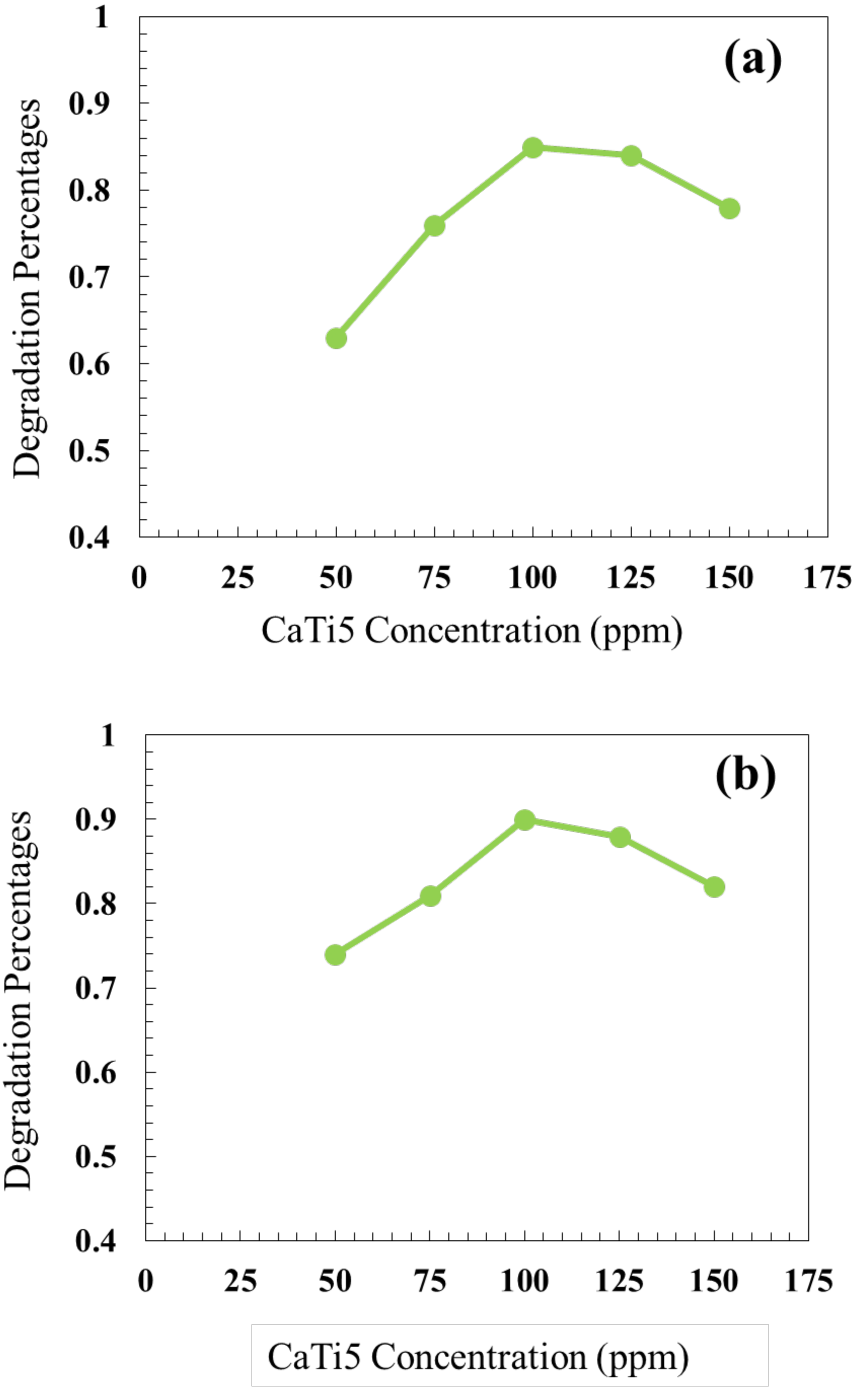

Fig. 11. Influence of catalyst loading on the performance of Ca-doped TiO_2 photocatalysts in degradation of (a) MB and (b) RhB.

On the one hand, the holes (h^+) oxidize the adsorbed water molecules or the hydroxyl anions (OH^-) and organic pollutants (R) on the surface of the photocatalyst to generate hydroxyl radicals. Moreover, superoxide radicals $O_2^{\bullet -}$ could be formed by direct interaction of electrons and oxygen, or other electron acceptors [47, 48]. These processes are illustrated in the following Eqs. 4-8.

$$H_2O_{ads} + h^+ \rightarrow H^+ + HO^\bullet{}_{ads} \quad (4)$$

$$HO^-{}_{ads} + h^+ \rightarrow HO^\bullet{}_{ads} \quad (5)$$

$$R_{ads} + h^+ \rightarrow R^\bullet{}_{ads} \quad (6)$$

$$O_2 + e^- \rightarrow O_2^{\bullet -} \quad (7)$$

$$Ca\text{-}TiO_2 + e^-_{BC} + h^+_{BV} \rightarrow Ca\text{-}TiO_2 \quad (8)$$

The total degradation pathway of any R is represented in Eq. 8. Indeed, the created hydroxyl radicals (•OH) and oxygen during the photocatalytic processes are mainly responsible for the degradation of any R, including dyes.

$$\text{Dyes} + HO^\bullet \rightarrow \text{Degradation Product} \quad (9)$$

Kwi J et al. [49] reported that anatase TiO_2 surface in the face of organic matter and O_2 has better adsorption capacity than rutile TiO_2, because photoacoustic electrons and holes are not easy to compound in anatase TiO_2. Ca^{2+} doping increases the transformation of amorphous TiO_2 to anatase phase, which increases the ratio of anatase TiO_2 in the TiO_2, and improves the photocatalytic efficiency catalyst. Luan Yong et al. [27] reported that metal ions can be used as an electron capture agent to reduce the recombination of e^-/h^+ pairs and improve the photocatalytic efficiency of TiO_2. Ca^{2+} ions enter in lattice, substitute Ti^{4+} and induce oxygen vacancies, reduce the binding rate of the electron hole, improving the photocatalytic activity of TiO_2 photocatalysts. Ca^{2+} can play the role of electron capture agent on Ca-doped TiO_2, to promote the separation of electrons and holes by trapping electron, and improve the photocatalytic activity of catalysts [50].

Comparison of catalytic performance with literature

In this section, the results of this study were compared with other studies in the literature. The results of this comparison were summarized in Table 4. The amount of degradation for MB and RhB via utilization of CaTi5 after 240 min simulated sunlight illumination were 85% and 90%, respectively. Comparing these results with regarding to the light source, synthesis method and time of degradations, proved that synthesized photocatalysts in this study especially CaTi5 were presented the acceptable catalytic performances.

CONCLUSION

In this study, Ca-doped TiO_2 photocatalysts with various amounts of calcium (0, 3 and 5 wt. %) and also, utilization of Cannabis Sativa leaves were synthesized with green sol-gel technique. Subsequent, prepared photocatalysts were used for MB and RhB degradation. Among the prepared photocatalysts, CaTi5 presented superior physicochemical properties in comparison with the other ones. Noted properties were as follow: higher surface area, smaller particles size and uniform dispersion, higher ability to form of surface free radical (OH) and lower energy band gap. Owing to the above mentioned excellent characterizations, the greatest amount of dye degradation was found for CaTi5. Degradation efficiency of the MB and RhB for CaTi5 after 240 min test were 85% and 90%, respectively. Moreover, the results proved that the reaction of photocatalytic dyes degradation followed by the pseudo first-order reaction kinetic. Furthermore, the effect of photocatalysts concentration on the degradation efficiency was evaluated with utilization of various concentrations of CaTi5 (50, 75, 100, 125 and 150 ppm). The highest amount of dyes degradation was found for 100 ppm catalyst concentration. However, the results evidenced that increasing of Ca loadings caused the superior catalytic activity, but agglomeration, pore blockage, lower surface area and subsequently lower photocatalytic activity were possible for higher calcium loadings (more than 5 wt.%). Therefore, we can say that addition of a lower amount of Ca to the pure TiO_2 is appropriate and led to the better characterization and higher photocatalytic activity.

CONFLICT OF INTEREST

The authors declare that there is no conflict of interests regarding the publication of this manuscript.

REFERENCES

1. Villanueva CM, Evlampidou I, Ibrahim F, Donat-Vargas C, Valentin A, Tugulea A-M, et al. Global assessment of chemical quality of drinking water: The case of trihalomethanes. Water Res. 2023;230:119568-119568.
2. Ahmed MA, Mohamed AA. Recent progress in semiconductor/graphene photocatalysts: synthesis, photocatalytic applications, and challenges. RSC advances. 2022;13(1):421-439.
3. waghchaure RH. Photocatalytic Degradation of Methylene Blue, Rhodamine B, Methyl Orange and Eriochrome Black T Dyes by Modified Zno Nanocatalysts: A Concise Review. SSRN Electronic Journal. 2022.
4. Tahir MB, Rafique M, Sagir M, Ullah S, Kiran H, Nawaz T. Role of Nanomaterials in the Detoxification of Harmful Dyes. Encyclopedia of Smart Materials: Elsevier; 2022. p. 373-386.
5. Berradi M, Hsissou R, Khudhair M, Assouag M, Cherkaoui O, El Bachiri A, et al. Textile finishing dyes and their impact on aquatic environs. Heliyon. 2019;5(11):e02711-e02711.
6. Kishor R, Purchase D, Saratale GD, Saratale RG, Ferreira LFR, Bilal M, et al. Ecotoxicological and health concerns of persistent coloring pollutants of textile industry wastewater and treatment approaches for environmental safety. Journal of Environmental Chemical Engineering. 2021;9(2):105012.
7. Ruan W, Hu J, Qi J, Hou Y, Zhou C, Wei X. Removal of dyes from wastewater by nanomaterials : A review. Advanced Materials Letters. 2019;10(1):9-20.
8. Zarrabi M, Haghighi M, Alizadeh R. Sonoprecipitation dispersion of ZnO nanoparticles over graphene oxide used in photocatalytic degradation of methylene blue in aqueous solution: Influence of irradiation time and power. Ultrason Sonochem. 2018;48:370-382.
9. Zhang F, Wang X, Liu H, Liu C, Wan Y, Long Y, et al. Recent Advances and Applications of Semiconductor Photocatalytic Technology. Applied Sciences. 2019;9(12):2489.
10. Gautam S, Agrawal H, Thakur M, Akbari A, Sharda H, Kaur R, et al. Metal oxides and metal organic frameworks for the photocatalytic degradation: A review. Journal of Environmental Chemical Engineering. 2020;8(3):103726.
11. Ncibi MC, Mahjoub B, Seffen M. Adsorptive removal of textile reactive dye using Posidonia oceanica (L.) fibrous biomass. International Journal of Environmental Science and Technology. 2007;4(4):433-440.
12. Ge J, Zhang Y, Heo Y-J, Park S-J. Advanced Design and Synthesis of Composite Photocatalysts for the Remediation of Wastewater: A Review. Catalysts. 2019;9(2):122.
13. Kong EDH, Chau JHF, Lai CW, Khe CS, Sharma G, Kumar A, et al. GO/ TiO_2-Related Nanocomposites as Photocatalysts for Pollutant Removal in Wastewater Treatment. Nanomaterials (Basel, Switzerland). 2022;12(19):3536.
14. Chakraborty A, Samriti, Ruzimuradov O, Gupta RK, Cho J, Prakash J. TiO_2 nanoflower photocatalysts: Synthesis, modifications and applications in wastewater treatment for removal of emerging organic pollutants. Environ Res. 2022;212:113550.
15. Bakardjieva S, Stengl V, Szatmary L, Subrt J, Lukac J, Murafa N, et al. Transformation of brookite-type TiO_2 nanocrystals to rutile: correlation between microstructure and photoactivity. J Mater Chem. 2006;16(18):1709.
16. Asadi A, Akbarzadeh R, Eslami A, Jen T-C, Ozaveshe Oviroh P. Effect of synthesis method on NS-TiO_2 photocatalytic performance. Energy Procedia. 2019;158:4542-4547.
17. Basu S, Saha S. Effect of synthesis method on the photocatalytic activity of TiO_2 nanoparticles. AIP Conference Proceedings: Author(s); 2019. p. 020003.
18. Riazian M, Bahari A. Synthesis and nanostructural investigation of TiO2 nanorods doped by SiO_2. Pramana. 2011;78(2):319-331.
19. Tseng H-H, Wei M-C, Hsiung S-F, Chiou C-W. Degradation of xylene vapor over Ni-doped TiO_2 photocatalysts prepared by polyol-mediated synthesis. Chem Eng J. 2009;150(1):160-167.
20. Devi LG, Kottam N, Murthy BN, Kumar SG. Enhanced photocatalytic activity of transition metal ions Mn2+, Ni2+ and Zn^{2+} doped polycrystalline titania for the degradation of Aniline Blue under UV/solar light. J Mol Catal A: Chem. 2010;328(1-2):44-52.
21. Zhu J, Deng Z, Chen F, Zhang J, Chen H, Anpo M, et al. Hydrothermal doping method for preparation of Cr^{3+}-TiO_2 photocatalysts with concentration gradient distribution of Cr^{3+}. Applied Catalysis B: Environmental. 2006;62(3-4):329-335.
22. Asahi R, Morikawa T, Irie H, Ohwaki T. Nitrogen-Doped Titanium Dioxide as Visible-Light-Sensitive Photocatalyst: Designs, Developments, and Prospects. Chem Rev. 2014;114(19):9824-9852.
23. Asahi R, Morikawa T, Ohwaki T, Aoki K, Taga Y. Visible-Light Photocatalysis in Nitrogen-Doped Titanium Oxides. Science. 2001;293(5528):269-271.
24. Liu S, Wang C, Song Y, Yan B, Ai B, Pan K, et al. Fabrication of a hybrid phase TiO_2/g-C_3N_4 heterojunction composite with enhanced adsorption and photocatalytic degradation of MB under visible light. New J Chem. 2023;47(17):8170-8181.
25. Basumatary B, Basumatary R, Ramchiary A, Konwar D. Evaluation of Ag@ TiO_2/WO_3 heterojunction photocatalyst for enhanced photocatalytic activity towards methylene blue degradation. Chemosphere. 2022;286:131848.
26. Malik R, Tomer VK, Duhan S, Rana PS, Nehra SP. Facile Preparation of TiO_2-SnO_2 Catalysts using TiO_2 as an Auxiliary for Gas Sensing and Advanced Oxidation Processes. MRS Advances. 2016;1(46):3157-3162.
27. Yu J, Wang W, Cheng B. Synthesis and Enhanced Photocatalytic Activity of a Hierarchical Porous Flowerlike p–n Junction NiO/ TiO_2 Photocatalyst. Chemistry – An Asian Journal. 2010;5(12):2499-2506.
28. Teng Q, Zhou X, Jin B, Luo J, Xu X, Guan H, et al. Synthesis and enhanced photocatalytic activity of a BiOI/ TiO_2 nanobelt array for methyl orange degradation under visible light irradiation. RSC Advances. 2016;6(43):36881-36887.
29. Verma V, Al-Dossari M, Singh J, Rawat M, Kordy MGM, Shaban M. A Review on Green Synthesis of TiO_2 NPs: Photocatalysis and Antimicrobial Applications. Polymers. 2022;14(7):1444.
30. Amjad R, Mubeen B, Ali SS, Imam SS, Alshehri S, Ghoneim MM, et al. Green Synthesis and Characterization of Copper Nanoparticles Using Fortunella margarita Leaves. Polymers. 2021;13(24):4364.

31. Jayapriya M, Arulmozhi M. Beta vulgaris peel extract mediated synthesis of Ag/TiO_2 nanocomposite: Characterization, evaluation of antibacterial and catalytic degradation of textile dyes-an electron relay effect. Inorg Chem Commun. 2021;128:108529.
32. Bopape DA, Mathobela S, Matinise N, Motaung DE, Hintsho-Mbita NC. Green Synthesis of CuO-TiO_2 Nanoparticles for the Degradation of Organic Pollutants: Physical, Optical and Electrochemical Properties. Catalysts. 2023;13(1):163.
33. Ahmad MM, Mushtaq S, Al Qahtani HS, Sedky A, Alam MW. Investigation of TiO_2 Nanoparticles Synthesized by Sol-Gel Method for Effectual Photodegradation, Oxidation and Reduction Reaction. Crystals. 2021;11(12):1456.
34. Liu C, Yu K, Zhang Y, Zhu X, He F, Eliasson B. Characterization of plasma treated Pd/HZSM-5 catalyst for methane combustion. Applied Catalysis B: Environmental. 2004;47(2):95-100.
35. Sajjadi SM, Haghighi M. Combustion vs. hybrid sol-gel-plasma surface design of coke-resistant Co-promoted Ni-spinel nanocatalyst used in combined reforming of CH_4/CO_2/O_2 for hydrogen production. Chem Eng J. 2019;362:767-782.
36. Gonzalez RD, Lopez T, Gomez R. Sol—Gel preparation of supported metal catalysts. Catal Today. 1997;35(3):293-317.
37. Mohtar SS, Aziz F, Ismail AF, Sambudi NS, Abdullah H, Rosli AN, et al. Impact of Doping and Additive Applications on Photocatalyst Textural Properties in Removing Organic Pollutants: A Review. Catalysts. 2021;11(10):1160.
38. Sajjadi SM, Haghighi M, Fard SG, Eshghi J. Various calcium loading and plasma-treatment leading to controlled surface segregation of high coke-resistant Ca-promoted NiCo–$NiAl_2O_4$ nanocatalysts employed in CH4/CO2/O2 reforming to H2. Int J Hydrogen Energy. 2022;47(59):24708-24727.
39. Čolović B, Kisić D, Jokanović B, Rakočević Z, Nasov I, Petkoska AT, et al. Wetting properties of titanium oxides, oxynitrides and nitrides obtained by DC and pulsed magnetron sputtering and cathodic arc evaporation. Materials Science-Poland. 2019;37(2):173-181.
40. Sajjadi SM, Haghighi M, Rahmani F, Eshghi J. Plasma-enhanced sol-gel fabrication of $CoWNiAl_2O_4$ nanocatalyst used in oxidative conversion of greenhouse CH_4/CO_2 gas mixture to H_2/CO. Journal of CO_2 Utilization. 2022;61:102037.
41. Ajamein H, Haghighi M. On the microwave enhanced combustion synthesis of CuO–ZnO–Al_2O_3 nanocatalyst used in methanol steam reforming for fuel cell grade hydrogen production: Effect of microwave irradiation and fuel ratio. Energy Convers Manage. 2016;118:231-242.
42. Daghrir R, Drogui P, Robert D. Modified TiO_2 For Environmental Photocatalytic Applications: A Review. Industrial & Engineering Chemistry Research. 2013;52(10):3581-3599.
43. Tian G, Fu H, Jing L, Tian C. Synthesis and photocatalytic activity of stable nanocrystalline TiO_2 with high crystallinity and large surface area. J Hazard Mater. 2009;161(2-3):1122-1130.
44. Arshad Z, Shakir S, Khoja AH, Javed AH, Anwar M, Rehman A, et al. Performance Analysis of Calcium-Doped Titania (TiO_2) as an Effective Electron Transport Layer (ETL) for Perovskite Solar Cells. Energies. 2022;15(4):1408.
45. Harikishore M, Sandhyarani M, Venkateswarlu K, Nellaippan TA, Rameshbabu N. Effect of Ag Doping on Antibacterial and Photocatalytic Activity of Nanocrystalline TiO_2. Procedia Materials Science. 2014;6:557-566.
46. Liu S, Min Z, Hu D, Liu Y. Synthesis of Calcium Doped TiO_2 Nanomaterials and Their Visible Light Degradation Property. Advances in Intelligent Systems Research: Atlantis Press; 2014.
47. Ejhieh AN, Khorsandi M. Photodecolorization of Eriochrome Black T using NiS–P zeolite as a heterogeneous catalyst. J Hazard Mater. 2010;176(1-3):629-637.
48. Tóth J. Calculation of the BET-Compatible Surface Area from Any Type I Isotherms Measured above the Critical Temperature. J Colloid Interface Sci. 2000;225(2):378-383.
49. Kiwi J, Morrison C. Heterogeneous photocatalysis. Dynamics of charge transfer in lithium-doped anatase-based catalyst powders with enhanced water photocleavage under ultraviolet irradiation. The Journal of Physical Chemistry. 1984;88(25):6146-6152.
50. Minchi L, Cao F, Xinni Z, Youqiang C, Xuhua L. Photocatalytic activity of Ca-TiO_2 nanofibers with different concentrations of calcium. Chem Phys Lett. 2019;736:136807.
51. Ramzan M, Obodo RM, Shahzad MI, Mukhtar S, Ilyas SZ, Mahmood T. Green synthesis of Cu@TiO_2 via cedrus deodara leaf extract: A novel composite with high photocatalytic and antibacterial activity. Current Research in Green and Sustainable Chemistry. 2021;4:100137.
52. Nassoko D, Li Y-F, Li J-L, Li X, Yu Y. Neodymium-Doped TiO_2 with Anatase and Brookite Two Phases: Mechanism for Photocatalytic Activity Enhancement under Visible Light and the Role of Electron. International Journal of Photoenergy. 2012;2012:1-10.
53. Hassan SM, Ahmed AI, Mannaa MA. Surface acidity, catalytic and photocatalytic activities of new type $H_3PW_{12}O_{40}$/Sn-TiO_2 nanoparticles. Colloids Surf Physicochem Eng Aspects. 2019;577:147-157.
54. Sun W, Zhang S, Liu Z, Wang C, Mao Z. Studies on the enhanced photocatalytic hydrogen evolution over Pt/PEG-modified TiO2 photocatalysts. Int J Hydrogen Energy. 2008;33(4):1112-1117.
55. Kunnamareddy M, Rajendran R, Sivagnanam M, Rajendran R, Diravidamani B. Nickel and sulfur codoped TiO_2 nanoparticles for efficient visible light photocatalytic activity. Journal of Inorganic and Organometallic Polymers and Materials. 2021;31(6):2615-2626.
56. Li Y-F, Zhong Y, Chang J-Q, Hu C-H. Synthesis and effects on visible light photocatalytic activity of $Bi_2Ti_2O_7$ photocatalyst. IOP Conference Series: Materials Science and Engineering. 2018;307:012041.
57. Abbasi Asl E, Haghighi M, Talati A. Sono-solvothermal fabrication of flowerlike $Bi_7O_9I_3$-$MgAl_2O_4$ p-n nano-heterostructure photocatalyst with enhanced solar-light-driven degradation of methylene blue. Solar Energy. 2019;184:426-439.
58. Abbasi E, Haghighi M, Shokrani R, Shabani M. Copper plasmon-induced Cu-doped ZnO-CuO double-nanoheterojunction: In-situ combustion synthesis and photo-decontamination of textile effluents. Mater Res Bull. 2020;129:110880.
59. Somraksa W, Suwanboon S, Amornpitoksuk P, Randorn C. Physical and Photocatalytic Properties of CeO_2/ZnO/$ZnAl_2O_4$ Ternary Nanocomposite Prepared by Co-precipitation Method. Materials Research. 2020;23(1).